JOURNAL OF THERMOPHYSICS AND HEAT TRANSFER
Vol. 23, No. 4, October–December 2009

Free Convection About a Vertical Circular Plate

S. C. Haldar*
University of the West Indies at St. Augustine, Trinidad, Trinidad and Tobago, West Indies

DOI: 10.2514/1.38589

This paper reports on a study of a three-dimensional numerical solution of free convection of air about a vertical circular plate for isothermal and isoflux heating conditions. The governing equations were solved in a vorticity and vector potential formulation. Fluid is drawn toward the heated plate from the bottom and the front of it. The fluid converges as it approaches the plate and moves almost vertically upward close to the plate. For the case of isoflux heating, the plate temperature at a particular radius increases with height and the location of maximum temperature shifts upward with increasing Grashof number. For both isothermal and isoflux heating conditions, the correlations between the Nusselt and Grashof numbers for the case of the circular plate have been developed as a function of the same for the flat plate under similar conditions.

Nomenclature

g^*	=	acceleration due to gravity, m s^{-2}
Gr	=	Grashof number, $g^*\beta^* T^*_{\text{ref}} L^{*3}_{\text{ref}}/\nu^{*2}$
k^*	=	thermal conductivity, W · m^{-1} · K^{-1}
L^*	=	height of flat plate, m, 1
L^*_{ref}	=	reference length, m, L^* for the flat plate and r^*_p for the circular plate
Nu	=	average Nusselt number, $h^* L^*_{\text{ref}}/k^*$
Pr	=	Prandtl number
q^*	=	heat flux, W · m^{-2}
r^*	=	radial coordinate, m, Fig. 1, r^*/r^*_P
r^*_P	=	plate radius, m, 1.0
Ra	=	Rayleigh number, $Gr \times Pr$
T^*	=	temperature, K, $(T^* - T^*_\infty)/T^*_{\text{ref}}$
T^*_{ref}	=	reference temperature, K, $(T^*_P - T^*_\infty)$ for the isothermal plate and $q^* L^*_{\text{ref}}/k^*$ for the isoflux plate
T^*_∞	=	freestream temperature, K, 0
$u*$	=	velocity along r^*, m · s^{-1}, $u^*/(\nu^*/r^*_P)$
v^*	=	velocity along θ, m · s^{-1}, $v^*/(\nu^*/r^*_P)$
w^*	=	velocity along z^*, m · s^{-1}, $w^*/(\nu^*/r^*_P)$
z^*	=	axial coordinate, m, Fig. 1, z^*/r^*_P
β^*	=	coefficient of volumetric expansion, K^{-1}
θ	=	angular coordinate, Fig. 1
ν^*	=	kinematic viscosity, m^2 · s^{-1}
Ψ^*_r	=	r^* component of vector potential, m^2 · s^{-1}, Ψ^*_r/ν^*
Ψ^*_θ	=	θ component of vector potential, m^2 · s^{-1}, Ψ^*_θ/ν^*
Ψ^*_z	=	z^* component of vector potential, m^2 · s^{-1}, Ψ^*_z/ν^*
Ω^*_r	=	r^* component of vorticity, s^{-1}, $\Omega^*_r/(\nu^*/r^{*2}_p)$
Ω^*_θ	=	θ component of vorticity, s^{-1}, $\Omega^*_\theta/(\nu^*/r^{*2}_p)$
Ω^*_z	=	z^* component of vorticity, s^{-1}, $\Omega^*_z/(\nu^*/r^{*2}_p)$

Subscripts

∞	=	freestream
p	=	plate

Superscript

$*$	=	dimensional quantity

Received 16 May 2008; revision received 11 May 2009; accepted for publication 13 May 2009.

*Department of Mechanical and Manufacturing Engineering; schaldar@rediffmail.com.

I. Introduction

HEAT transfer by free convection is a common phenomenon in many natural and engineering processes. The rate of free convection heat transfer from a surface depends on its geometry as well as its orientation. Correlations between Nu and Gr or Ra are available in almost all books on heat transfer for various combinations of surface geometry and its orientation. Gebhart et al. [1] discussed many free convection problems and correlations. Free convection about a flat plate with a width much larger than its height, commonly referred to as flat plate, in vertical orientation has possibly received the widest attention amongst free convection studies. Most of these studies deal with the analytical solution of boundary-layer equations based on the assumption that the boundary layer begins at the leading edge of the plate. Because boundary-layer equations are parabolic in nature, the solution is not influenced by activities downstream. Consequently, the results are applicable away from the leading and trailing edges of a plate of finite height. Martynenko et al. [2] provided a list of a large number of early studies on this topic. They also attempted to address the leading-edge issue with the help of a deformed longitudinal coordinate. Yang and Yao [3] introduced a double-deck structure at the trailing edge to account for its effect. Wright and Gebhart [4] addressed the leading-edge effects with the inclusion of the region below the plate into the solution domain. The equations were solved on a plane of transformed coordinates, and the obtained flowfield was explained with the help of a motion pressure gradient. However, the paper does not provide results on the Nusselt number. Vynnycky and Kimura [5] considered the thickness of the plate as well and solved the problem as a conjugate one. In a relatively recent paper, Andreozzi et al. [6] solved the elliptic form of the Navier–Stokes and energy equations by including into the numerical solution the regions upstream and downstream of the plate. It may be mentioned here that Andreozzi et al. considered a plate with an isoflux condition whereas most of the previous investigations dealt with an isothermal plate. All the studies cited here assume a plate with a width much larger than its height, rendering the problem two dimensional. A free convection about a circular plate oriented vertically has the additional difficulty of a three-dimensional nature. The author is not aware of any study on this topic, though it is one of the more commonly encountered geometries, such as the two ends of a cylindrical boiler drum or other storage vessel and the casing of electric motors. The present paper attempts to fill this gap in the literature.

II. Problem Description and Governing Equations

Figure 1 presents the schematic of the physical problem and the coordinate directions with the respective velocity components. The surface is flat, circular, and oriented vertically and is surrounded by an infinite medium of quiescent air. Because of the symmetry of the problem about the vertical plane passing through the plate center,

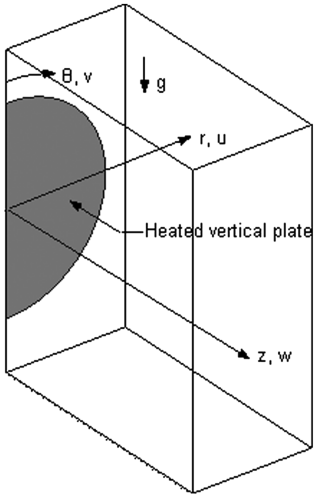

Fig. 1 Schematic of the problem with coordinate directions and velocity components.

only one-half of the physical domain has been taken into consideration. Two cases of the heated plate were considered: isothermal and isoflux.

The equations governing the fluid flow have been expressed in a vorticity-vector potential formulation, which is an extension of a vorticity-stream function formulation in two dimensions. It may be mentioned here that stream function is not defined for three-dimensional flows. The three components of the vorticity-transport equation in cylindrical polar coordinates under Boussinesq's approximation take the following forms when expressed in dimensionless variables as defined in the nomenclature:

$$\frac{1}{r}\frac{\partial(ur\Omega_r)}{\partial r}+\frac{1}{r}\frac{\partial(v\Omega_r)}{\partial\theta}+\frac{\partial(w\Omega_r)}{\partial z}-\left[\frac{1}{r}\frac{\partial(ur\Omega_r)}{\partial r}+\frac{1}{r}\frac{\partial(u\Omega_\theta)}{\partial\theta}+\frac{\partial(u\Omega_z)}{\partial z}\right]=\left[\frac{\partial^2\Omega_r}{\partial r^2}+\frac{1}{r}\frac{\partial\Omega_r}{\partial r}+\frac{1}{r^2}\frac{\partial^2\Omega_r}{\partial\theta^2}+\frac{\partial^2\Omega_r}{\partial z^2}-\frac{\Omega_r}{r^2}-\frac{2}{r^2}\frac{\partial\Omega_\theta}{\partial\theta}\right]+Gr.\mathrm{Sin}\theta\frac{\partial T}{\partial z} \tag{1}$$

$$\frac{\partial(u\Omega_\theta)}{\partial r}+\frac{1}{r}\frac{\partial(v\Omega_\theta)}{\partial\theta}+\frac{\partial(w\Omega_\theta)}{\partial z}-\left[\frac{\partial(v\Omega_r)}{\partial r}+\frac{1}{r}\frac{\partial(v\Omega_\theta)}{\partial\theta}+\frac{\partial(v\Omega_z)}{\partial z}\right]=\left[\frac{\partial^2\Omega_\theta}{\partial r^2}+\frac{1}{r}\frac{\partial\Omega_\theta}{\partial r}+\frac{1}{r^2}\frac{\partial^2\Omega_\theta}{\partial\theta^2}+\frac{\partial^2\Omega_\theta}{\partial z^2}-\frac{\Omega_\theta}{r^2}+\frac{2}{r^2}\frac{\partial\Omega_r}{\partial\theta}\right]+Gr.\mathrm{Cos}\theta\frac{\partial T}{\partial z} \tag{2}$$

$$\frac{1}{r}\frac{\partial(ur\Omega_z)}{\partial r}+\frac{1}{r}\frac{\partial(v\Omega_z)}{\partial\theta}+\frac{\partial(w\Omega_z)}{\partial z}-\left[\frac{1}{r}\frac{\partial(wr\Omega_r)}{\partial r}+\frac{1}{r}\frac{\partial(w\Omega_\theta)}{\partial\theta}+\frac{\partial(w\Omega_z)}{\partial z}\right]=\left[\frac{\partial^2\Omega_z}{\partial r^2}+\frac{1}{r}\frac{\partial\Omega_z}{\partial r}+\frac{1}{r^2}\frac{\partial^2\Omega_z}{\partial\theta^2}+\frac{\partial^2\Omega_z}{\partial z^2}\right]-Gr\left[\mathrm{Sin}\theta\frac{\partial T}{\partial r}+\frac{\mathrm{Cos}\theta}{r}\frac{\partial T}{\partial\theta}\right] \tag{3}$$

The relationships between the velocity and vector potential need to be such that they satisfy the continuity equation and, accordingly,

$$u=\frac{1}{r}\frac{\partial\Psi_z}{\partial\theta}-\frac{\partial\Psi_\theta}{\partial z} \tag{4}$$

$$v=\frac{\partial\Psi_r}{\partial z}-\frac{\partial\Psi_z}{\partial r} \tag{5}$$

and

$$w=\frac{1}{r}\frac{\partial(r\Psi_\theta)}{\partial r}-\frac{1}{r}\frac{\partial\Psi_r}{\partial\theta} \tag{6}$$

Now, Ψ_x, Ψ_y, and Ψ_z may be chosen to satisfy

$$\frac{1}{r}\frac{\partial(r\Psi r)}{\partial r}+\frac{1}{r}\frac{\partial\Psi_\theta}{\partial\theta}+\frac{\partial\Psi_z}{\partial z}=0 \tag{7}$$

With this, the three vorticity definition equations then reduce to

$$-\Omega_r=\frac{\partial^2\Psi_r}{\partial r^2}+\frac{1}{r}\frac{\partial\Psi_r}{\partial r}+\frac{1}{r^2}\frac{\partial^2\Psi_r}{\partial\theta^2}+\frac{\partial^2\Psi_r}{\partial z^2}-\frac{2}{r^2}\frac{\partial\Psi_\theta}{\partial\theta}-\frac{\Psi_r}{r^2} \tag{8}$$

$$-\Omega_\theta=\frac{\partial^2\Psi_\theta}{\partial r^2}+\frac{1}{r}\frac{\partial\Psi_\theta}{\partial r}+\frac{1}{r^2}\frac{\partial^2\Psi_\theta}{\partial\theta^2}+\frac{\partial^2\Psi_\theta}{\partial z^2}+\frac{2}{r^2}\frac{\partial\Psi_z}{\partial\theta}-\frac{\Psi_\theta}{r^2} \tag{9}$$

$$-\Omega_z=\frac{\partial^2\Psi_z}{\partial r^2}+\frac{1}{r}\frac{\partial\Psi_z}{\partial r}+\frac{1}{r^2}\frac{\partial^2\Psi_z}{\partial\theta^2}+\frac{\partial^2\Psi_z}{\partial z^2} \tag{10}$$

The energy equation in dimensionless form reads as

$$\frac{1}{r}\frac{\partial(urT)}{\partial r}+\frac{1}{r}\frac{\partial(vT)}{\partial\theta}+\frac{\partial(wT)}{\partial z}=\frac{1}{Pr}\left[\frac{\partial^2T}{\partial r^2}+\frac{1}{r}\frac{\partial T}{\partial r}+\frac{1}{r^2}\frac{\partial^2T}{\partial\theta^2}+\frac{\partial^2T}{\partial z^2}\right] \tag{11}$$

For the numerical investigation of three-dimensional flow and heat transfer problems, the governing equations have been dealt with most commonly in primitive variables. Amongst a few works on vorticity-vector potential formulation in cylindrical polar coordinates, the one by Tolpadi and Kuehn [7] that deals with free convection about a horizontal cylinder attached with annular fins may be cited here.

III. Boundary Conditions

The surfaces, real and imaginary, bounding the computational domain have been shown in Fig. 2. A coaxial horizontal pseudo-cylinder with a radius much larger than that of the plate was considered as one of the bounding surfaces to facilitate numerical computation. At one vertical end of this horizontal cylinder lies the heated plate, whereas the free end on the opposite side provided another boundary surface. These two imaginary boundaries, the cylinder and the free circular vertical end, were positioned far enough apart from the plate so that their influences on the results were negligible. The heated plate occupies the circular vertical end of the

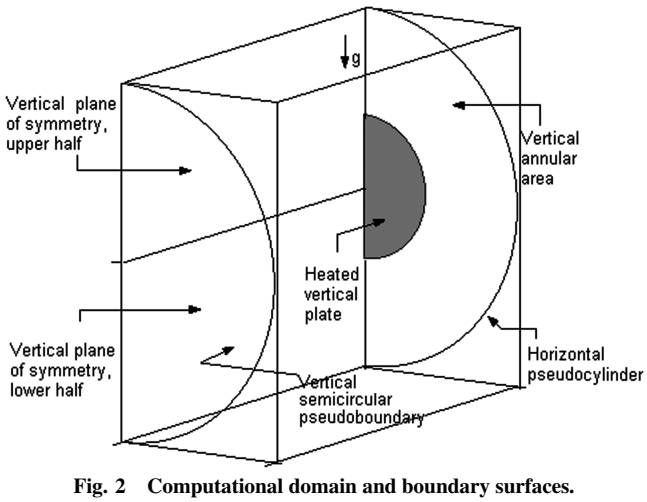

Fig. 2 Computational domain and boundary surfaces.

pseudocylinder only partially, and the remaining annular portion was deemed symmetric about the z axis. The fluid flow was assumed perpendicular across the pseudocylinder as well as the free vertical circular end opposite to the plate. The problem is symmetric about the vertical plane passing through the center of the plate; hence, the governing equations were solved in one-half of the domain to take advantage of the reduction in computation time. Equations (1–3) require conditions on Ω_r, Ω_θ, and Ω_z; Eqs. (8–10) on Ψ_r, Ψ_θ, and Ψ_z; and Eq. (11) on T at all the bounding surfaces to solve these coupled equations.

A. Horizontal Pseudocylinder

The fluid is deemed to cross the pseudocylinder orthogonally, which is radial for this boundary. The absence of axial and tangential velocity components yields $\Psi_r = -\frac{\partial^2 \Psi_r}{\partial r^2} = 0$, $\frac{\partial (r\Psi_\theta)}{\partial r} = 0$, and $\frac{\partial \Psi_z}{\partial r} = 0$ as the conditions for vector potential, and $\Omega_r = \frac{\partial \Omega_\theta}{\partial r} = \frac{\partial \Omega_z}{\partial r} = 0$ for the three components of vorticity. The fluid enters the domain with the temperature of the far-off ambient and, accordingly, $T = 0$ when $u < 0$ (inflow), whereas the condition $\frac{\partial T}{\partial r} = 0$ applies when $u > 0$, that is, to the fluid leaving the domain through this boundary.

B. Vertical End Containing the Plate

This boundary surface needs to be divided into two, the plate and the remaining free annular area, for the sake of specifying the conditions.

For the heated plate, $0 \le r \le 1$ and $0 \le \theta \le \pi$, no-slip condition results to $\Psi_r = \frac{\partial \Psi_r}{\partial z} = 0$, $\Psi_\theta = \frac{\partial \Psi_\theta}{\partial r} = 0$, $\Psi_z = \frac{\partial \Psi_z}{\partial r} = \frac{\partial^2 \Psi_z}{\partial \Psi_z^2} = 0$, and for vorticity $\Omega_r = -\frac{\partial^2 \Psi_r}{\partial z^2}$, $\Omega_\theta = -\frac{\partial^2 \Psi_\theta}{\partial z^2}$ and $\Omega_z = 0$. The case of the isothermal plate is specified by $T = 1.0$ and the isoflux by $\frac{\partial T}{\partial z} = -1$. It may be noted here that the reference temperatures for the two cases are different, as shown in the Nomenclature.

The remaining portion of this boundary, $1 < r$ and $0 \le \theta \le \pi$, was deemed symmetric about the z axis and, accordingly, $\Psi_r = \Psi_\theta = \frac{\partial \Psi_z}{\partial z} = 0$, $\Omega_r = \Omega_\theta = \frac{\partial \Omega_z}{\partial z} = 0$, and $\frac{\partial T}{\partial z} = 0$.

C. Free Vertical End Opposite to the Plate

The fluid is considered to cross this imaginary surface in the (r, θ) plane orthogonally, which is axial. Consequently, $\frac{\partial \Psi_r}{\partial z} = 0$, $\frac{\partial (r\Psi_\theta)}{\partial z} = 0$, $\Psi_z = -\frac{\partial^2 \Psi_z}{\partial z^2} = 0$, and $\frac{\partial \Omega_r}{\partial z} = \frac{\partial \Omega_\theta}{\partial z} = \Omega_z = 0$. The fluid enters $(w < 0)$ with $T = 0$ and leaves $(w > 0)$ with $\frac{\partial T}{\partial z} = 0$.

D. Upper ($\theta = 0$) and Lower ($\theta = \pi$) Vertical Planes of Symmetry

It is quite obvious that the problem is θ symmetric about the vertical plane passing through the plate center, and this yields to $\Psi_r = \frac{\partial \Psi_\theta}{\partial \theta} = \Psi_z = 0$, $\Omega_r = \frac{\partial \Omega_\theta}{\partial \theta} = \Omega_z = 0$, and $\frac{\partial T}{\partial \theta} = 0$ as the conditions on the upper and lower halves of this plane.

IV. Numerical Method

The governing dimensionless equations were solved by a finite difference technique based on control volume discretization over nonstaggered grids. The equations were discretized following the cell average QUICK scheme advocated by Leonard [8] to get rid of the instability associated with the central differencing scheme and the inaccuracy of the upwind scheme due to false diffusion at high flow velocities. However, central differencing was chosen for the wall adjacent control volumes.

Individual equations were deemed converged when the differences of the values of the respective variables between two consecutive iterations at each grid point were less than 0.001%, whereas the global convergence was considered achieved when the differences of vorticity values in the computational domain between two consecutive iteration cycles were less than 0.01%, where one cycle of iteration consists of the solution of Eqs. (1–3) for Ω_r, Ω_θ and Ω_z, respectively; Eqs. (8–10) for Ψ_x, Ψ_y, and Ψ_z; Eqs. (4–6) for u, v, and w from ψ_x, ψ_y, and ψ_z; and Eq. (11) for T.

For the purpose of validation, the code was reduced to the case of free convection about a horizontal isothermal cylinder. This is a two-dimensional (r, θ) problem, but it was solved as a three-dimensional one to maintain the three-dimensional nature of the code. The results obtained were found identical at all z locations and also in excellent agreement with those reported by Saito et al. [9].

The program was then run for the present topic of free convection about a circular plate to establish the locations of the two pseudoboundaries, the horizontal cylinder and the vertical circular end opposite to the heated plate, such that they would not influence the results. The distance of the two pseudoboundaries were gradually increased, and the changes in the plate average Nu values were found to be negligible when the radius of the horizontal cylinder was 2.5 or greater and the vertical circular boundary was located at a nondimensional distance of greater than 3.0 from the plate.

A grid-independence study was carried out by solving the governing equations with various values of grid spacing along the three coordinate directions. Velocity rather than the temperature values were found to be more sensitive to the grid size. Spacing along one coordinate direction was varied while keeping the other two constant, and the same was performed for each of the three coordinate directions. Representative results from this exercise have been furnished in Table 1. A spacing of 0.025 along the r coordinate up to the plate periphery and then a spacing of 0.05, a uniform angular grid of 3 deg along the θ direction, and 10 axial grids of size 0.01 adjacent to the heated plate followed by 60 grids of 0.05 along z coordinate were chosen to generate results reported here.

V. Results and Discussions

The numerical solution was performed in a PC equipped with a Pentium-IV CPU of clock speed 2.8 GHz; consequently, the computation time was very large due to the three-dimensional nature of the problem. Fortunately, the governing parameter is only Gr when the fluid around the heated plate is selected as air by specifying a Pr value of 0.7 in Eq. (11). The computation was carried out for Gr values between 10^2 and 10^6 with a multiplication factor of 10 for the two thermal conditions of the heated plate: isothermal and isoflux.

A. Flow Pattern

The velocity values near the heated plate are much larger than those farther away from it, and this large difference in values makes it difficult to present the velocity vectors within the whole computational domain. To overcome this, the vectors have been presented on a vertical (r, θ) plane at an axial distance of 0.125 from the plate and within the radius of the plate, that is, $0 \le r \le 1.0$ for the case of a plate with uniform flux, Fig. 3a. In Fig. 3b, the vectors on the (r, z) plane passing through $\theta = 60$ deg within the identical range of the r coordinate and $z < 0.6$ are presented. The z axis in Fig. 3b has been stretched out by 4 times with respect to the other coordinate directions for the sake of presentation; consequently, the velocity vectors appear longer along z. The fluid is drawn toward the heated plate from the bottom as well as from the front of the plate. As the flow approaches the plate, the direction gradually changes upward and becomes almost vertical close to the plate. The fluid finally leaves

Table 1 Changes in Nu with grid spacing for the isothermal circular plate at $Gr = 10^3$

Grid spacing and number of grids			Nu
Along r	Along θ	Along z	
$0.050 \times 20 + 0.05 \times 30$	3 deg $\times 60$	$0.0125 \times 10 + 0.05 \times 60$	6.4512
$0.025 \times 40 + 0.05 \times 30$	3 deg $\times 60$	$0.0125 \times 10 + 0.05 \times 60$	6.4826
$0.020 \times 50 + 0.05 \times 30$	3 deg $\times 60$	$0.0125 \times 10 + 0.05 \times 60$	6.4845
$0.025 \times 40 + 0.05 \times 30$	4 deg $\times 45$	$0.0125 \times 10 + 0.05 \times 60$	6.4939
$0.025 \times 40 + 0.05 \times 30$	2 deg $\times 90$	$0.0125 \times 10 + 0.05 \times 60$	6.4852
$0.025 \times 40 + 0.05 \times 30$	3 deg $\times 60$	0.05×62	6.5065
$0.025 \times 40 + 0.05 \times 30$	3 deg $\times 60$	$0.025 \times 10 + 0.05 \times 60$	6.4946
$0.025 \times 40 + 0.05 \times 30$	3 deg $\times 60$	$0.01 \times 10 + 0.05 \times 60$	6.4651

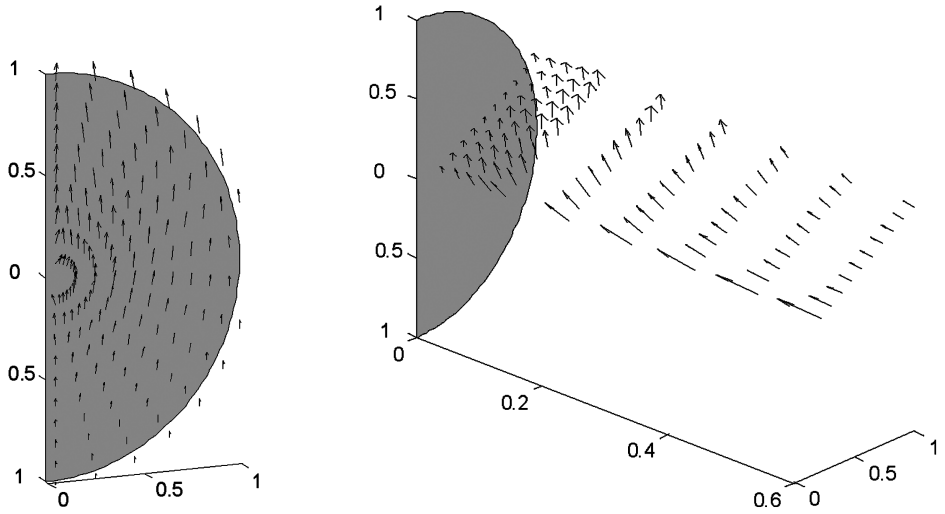

Fig. 3 Velocity vectors: a) vertical plane at $z = 0.125$, $Gr = 10^4$ for isoflux heating, and b) (r, z) plane at 60 deg for $Gr = 10^4$, isoflux plate.

the plate through a relatively smaller area at the periphery of the top half of the plate.

To investigate the angular regions of inflow and outflow, Fig. 4 plots the radial velocity at the plate periphery against the angular coordinate on a vertical plane close to the plate, $z = 0.1$, for the case of the isothermal plate. The positive segments of each profile indicate the outflow, whereas the negative segments represent the inflow through the bottom of the plate. The change of sign is approximately at $\theta = 90$ deg for all the profiles, indicating that the angular regions for inflow and outflow are shared almost equally. Apart from the inflow through the bottom of the plate, as represented by the negative segments of the profiles, the fluid is also drawn to the plate from its front. All the incoming fluid then converges and moves out through a relatively smaller area around the periphery of the top half of the plate, represented by the positive segments. This explains the large difference between the radial velocity values of the two segments of each profile.

B. Plate Temperature for Isoflux Heating

The temperature distribution over the plate losing heat with uniform flux is an important piece of information. Figure 5 presents this for $Gr = 10^6$. Each curve in the figure represents the angular variation of temperature at a particular radius. The dimensionless plate temperature at a particular radius gradually increases with height, with a steep increase adjacent to the upper vertical symmetry line. The maximum of each profile occurs at $\theta = 0$. The fluid temperature increases with height during its upward motion along the plate, and this necessitates the plate temperature to increase too, to transfer heat to the fluid with uniform flux.

The magnitude of the maximum plate temperature is useful for studying the development of hot spots. Figure 6 presents the dimensionless maximum temperature as a function of Gr and the corresponding correlation, $T_{\max} = 0.155\ Gr^{-0.164}$. The decreasing trend of maximum temperature with Gr is due to the definition of the reference temperature, $T^*_{\text{ref}} = q^* L^*_{\text{ref}}/k^*$, for isoflux heating. A careful look into the correlation will reveal that dimensional temperature, unlike dimensionless temperature, increases with Gr.

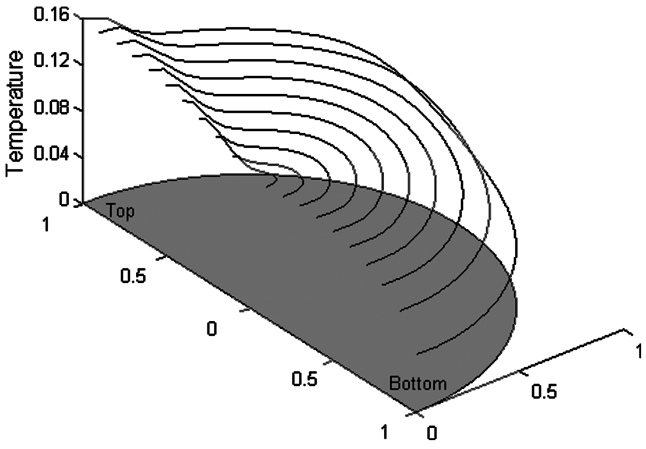

Fig. 5 Temperature variation over the isoflux plate, $Gr = 10^6$.

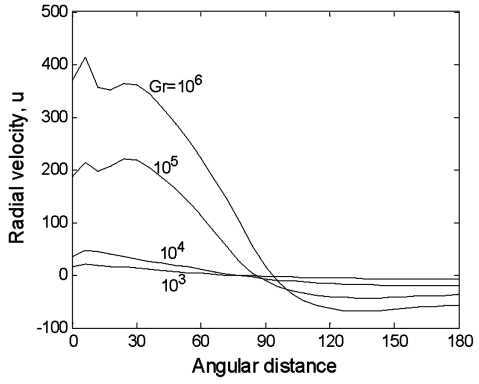

Fig. 4 Radial velocity at $r = 1.0$, $z = 0.1$ as a function of angle for the isothermal plate.

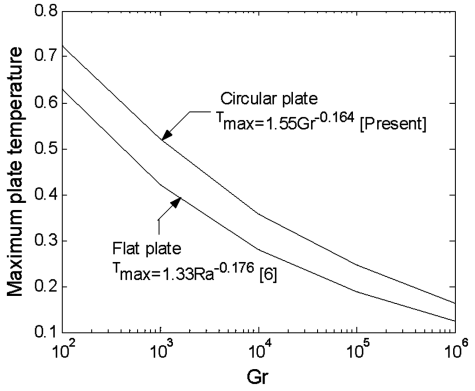

Fig. 6 Effect of Gr on the dimensionless maximum plate temperature for the isoflux case.

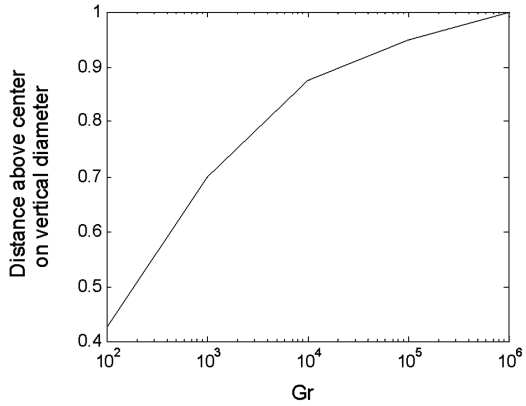

Fig. 7 Location of maximum temperature with *Gr* for the isoflux case.

The change of location of the maximum temperature on the plate with Gr is an interesting phenomenon to observe; see Fig. 7. The maximum temperature occurs exactly at the plate center if the heat transfer from the plate is purely due to conduction, $Gr = 0$. The onset of free convection shifts the location vertically upward on the symmetry line, and this trend continues with increasing Gr until it reaches the uppermost position of the plate at $Gr = 10^6$.

C. Air Temperature for Isothermal Plate

Figure 8 shows the variation of the air temperature along the axial line passing through the center of the plate (z axis) for the case of the isothermal plate for three values of Gr. Though the computational domain extends up to $z = 3.1$, the profile has been plotted up to $z = 1.25$ for the sake of clarity, especially close to the plate. At a lower Gr, say 10^2, the dominant mode of heat transfer is conduction; consequently, the temperature profile is nearly linear. With increasing Gr, the dominance of convection over conduction increases. Consequently, as Gr increases the fluid moves toward the plate with increasing velocity and this causes the temperature gradient at the plate to become steep. In other words, the axial distance through which the plate temperature is felt reduces with increasing Gr.

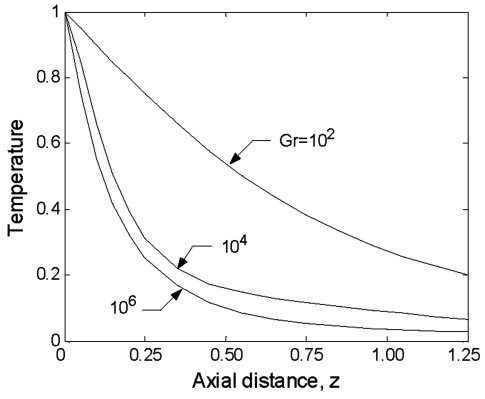

Fig. 8 Axial temperature variation along the z axis for the isothermal plate.

D. Nusselt Number

This is the parameter with the most practical importance in this investigation. The value of the Nusselt number at a location on the plate is a function of its r and θ coordinates. The Nu values averaged over the plate have been presented with Gr for the case of the isoflux plate in Fig. 9a and for the isothermal plate in Fig. 9b. The available correlations for the case of the flat plate and the corresponding profiles have been included in each figure for the sake of comparison. It may be recalled here that the reference length in the definition of Nu for flat plate is its height whereas, for the circular plate, it is its radius.

1. *Isoflux Plate*

For the case of the flat plate with isoflux condition, the two available correlations reproduced in Fig. 9a are almost identical for $Gr > 10^4$. The profile for the flat plate by Raithby and Hollands [10] and that for the circular plate obtained from the present study are almost parallel. Accordingly, the ratio of the flat plate Nu from [10] to that of the circular plate at a particular Gr was found to be nearly constant at 1.1. Thus, the Nu value for a vertical circular isoflux plate at a particular Gr may be estimated as (1/1.1) times the Nu value calculated for the flat plate from the corresponding correlation in [10]. The Nu values thus determined for the vertical circular plate deviate from those obtained numerically by a maximum of 2%.

For the sake of completeness, the correlation for the vertical flat plate by Raithby and Hollands [10] is reproduced here:

$$\bar{H}_l = \frac{6}{5}\left(\frac{Pr}{4 + 9\sqrt{Pr} + 10Pr}\right)^{1/5}, \qquad Nu^T = \bar{H}_l Ra^{1/5}$$

$$Nu_l = \frac{1.0}{\ell_n[1 + \frac{1.0}{Nu^T}]}, \qquad Nu_t = \frac{0.103^{3/4} Ra^{1/4}}{[1 + (\frac{7\times 10^{12} Pr}{Ra})^{0.4}]}$$

and, finally, $Nu = [Nu_l^m + Nu_t^m]^{1/m}$, where $m = 6.0$.

2. *Isothermal Plate*

Figure 9b presents the variation of Nu with Gr for the circular as well as the flat plate with isothermal heating condition. The corresponding correlation for the flat plate is reproduced here from [10]:

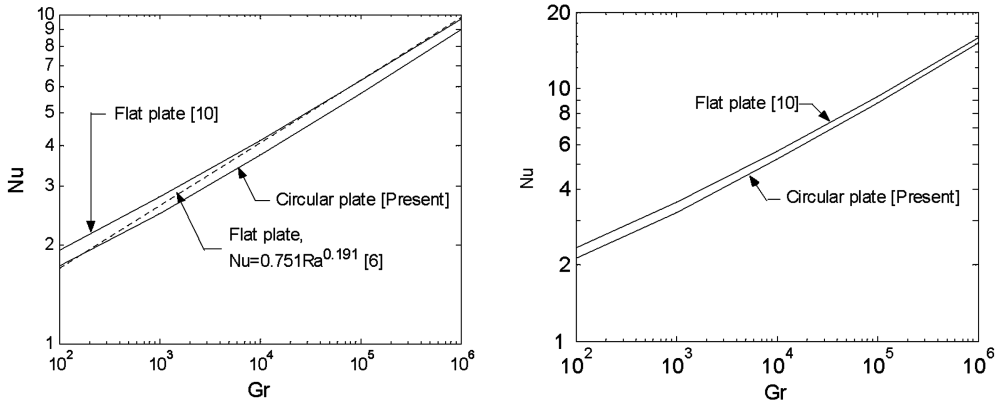

a) b)

Fig. 9 Variation of *Nu* with *Gr*: a) isoflux plate, and b) isothermal plate.

$$Nu^T = 0.515Ra^{1/4}, \qquad Nu_l = \frac{2.0}{\ell_n[1 + \frac{2.0}{Nu^T}]}$$

$$Nu_t = \frac{0.103Ra^{1/3}}{[1 + \frac{1.4\times10^9 Pr}{Ra}]} \quad \text{and} \quad Nu = [Nu_l^m + Nu_t^m]^{1/m}$$

with $m = 6.0$

.

The two curves converge at a very slow rate with increasing Gr, and this necessitates the ratio of the two Nu values at a particular Gr to be expressed as a function of Gr for better accuracy. It has been found that the Nu for a circular isothermal plate at a Gr is $(Gr^{0.005}/1.13)$ times its value for the flat plate. The proposed correlation for the circular plate deviates from the numerically generated Nu values by a maximum of less than 1%.

VI. Conclusions

This paper discusses the results from a three-dimensional numerical solution of laminar free convection about a vertical circular plate with uniform heat flux and uniform temperature conditions. The governing equations were rewritten in terms of vorticity and vector potentials. Two pseudosurfaces, a horizontal cylinder and the vertical circular end opposite to the heated plate, were considered as boundaries to facilitate numerical computation. Fluid was deemed to cross these imaginary boundaries orthogonally. The fluid is drawn toward the heated plate from the bottom as well as the front and then rises almost vertically close to the plate. For the case of uniform heat flux, the temperature of the circular plate at a radius increases from the bottom to the top, and the Nu value averaged over the plate was found to be (1/1.1) times of that of the flat plate, whereas for the circular plate with uniform temperature condition, the average Nu is $(Gr^{0.005}/1.13)$ times its value for the flat plate. The position of the maximum temperature for a plate losing heat with uniform flux shifts from the plate center for pure conduction to the topmost point on the plate periphery at $Gr = 10^6$.

References

[1] Gebhart, B., Jaluria, Y., Mahajan, R., and Sammakia, B., *Buoyancy-Induced Flows and Transport*, Hemisphere, Washington, D.C., 1988.

[2] Martynenko, O. G., Berezovsky, A. A., and Sokovishin, A., "Laminar Free Convection from a Vertical Plate," *International Journal of Heat and Mass Transfer*, Vol. 27, No. 6, 1984, pp. 869–881. doi:10.1016/0017-9310(84)90008-5

[3] Yang, R., and Yao, L. S., "Natural Convection Along a Finite Vertical Plate," *Journal of Heat Transfer*, Vol. 109, No. 2, 1987, pp. 413–418.

[4] Wright, N. T., and Gebhart, B., "The Entrainment Flow Adjacent to an Isothermal Vertical Surface," *International Journal of Heat and Mass Transfer*, Vol. 37, Suppl. 1, 1994, pp. 213–231. doi:10.1016/0017-9310(94)90023-X

[5] Vynnycky, M., and Kimura, S., "Conjugate Free Convection Due to a Heated Vertical Plate," *International Journal of Heat and Mass Transfer*, Vol. 39, No. 5, 1996, pp. 1067–1080. doi:10.1016/0017-9310(95)00188-3

[6] Andreozzi, A., Manca, O., and Morrone, B., "Numerical Solution to the Natural Convection on Vertical Isoflux Plates by Full Elliptic Equations," *Numerical Heat Transfer, Part A, Applications*, Vol. 41, 2002, pp. 263–283. doi:10.1080/10407780252780162

[7] Tolpadi, K., and Kuehn, T. H., "Computation of Conjugate Three-Dimensional Natural Convection Heat Transfer from a Transversely Finned Horizontal Cylinder," *Numerical Heat Transfer, Part A, Applications*, Vol. 16, 1989, pp. 1–13. doi:10.1080/10407788908944703

[8] Leonard, B. P., "Bounded Higher-Order Upwind Multidimensional Finite Volume Convection Diffusion Algorithms," *Advances in Numerical Heat Transfer*, edited by W. J. Minkowycz, and E. M. Sparrow, Vol. 1, Taylor and Francis, Philadelphia/London, 2000.

[9] Saito, T., Sajiki, T., and Muruhara, K., "Bench Mark Solutions to Natural Convection Heat Transfer Problem Around a Horizontal Circular Cylinder," *International Journal of Heat and Mass Transfer*, Vol. 36, No. 5, 1993, pp. 1251–1259. doi:10.1016/S0017-9310(05)80094-8

[10] Raithby, G. D., and Hollands, K. G. T., "Natural Convection," *Handbook of Heat Transfer*, edited by W. M. Rohsenow, J. P. Hartnett, and Y. I. Cho, 3rd ed., McGraw–Hill, New York, Chap. 4.